Measurement Notes

Note 66

February 2023

Experimental Measurements of High-Power Microwave (HPM) output from Relativistic A6 Magnetron at the University of New Mexico (UNM) for Directed Energy (DE) and non-DE applications

Andrey D. Andreev, Christopher Rodriguez, Michael Felix, and Edl Schamiloglu

University of New Mexico, Department of Electrical and Computer Engineering, Albuquerque, NM 87131

Abstract

The University of New Mexico (UNM) developed an A6 relativistic magnetron that may operate in two basic configurations of output power extraction from resonant cavities of the magnetron: (i) radial output with microwave power extraction from one of six resonant cavities into a rectangular horn antenna, and (ii) axial output microwave power extraction from all six resonant cavities smoothly tapered in the axial direction into a conical horn antenna. In both configurations, the magnetron is driven by the PULSERAD-110A electron beam accelerator that is able to provide 100's of kV of accelerating voltage and several kA of electron-beam current during tens of ns of output pulsed power with its internal output impedance ~35 Ω. While driven by kV/kA pulsed power, the A6 relativistic magnetron is able to provide 100's of MW of output microwave power either in the 2π-mode, whose "cold" operational frequency is ~4.6 GHz, or in the π-mode, whose "cold" operational frequency is ~2.3 GHz, with a standard solid cylindrical "cold" explosive-emission cathode. Results of latest experimental measurements of output microwave power from relativistic A6 magnetron with radial output in UNM demonstrated ~350 MW of HPM power at frequency ~4.675 GHz (2π-mode) during ~25 ns of output HPM pulse*

* This research was supported by AFOSR Grant FA9550-19-1-0225, AFOSR MURI Grant FA9550-20-1-0409, ONR Grants No. N00014-19-1-2155 and N00014-23-1-2072, and AFRL Cooperative Agreement FA9451-22-2-0016.

Natural synergy between fields of vacuum electronics and pulsed power has exhibited considerable progress during the last three decades resulting in tremendous achievements in high power electromagnetics (HPEM) and high-power microwave (HPM) applications [1]. The University of New Mexico (UNM) Applied Electromagnetics Group has been a leader in advancing intense electron-beam-driven HPM sources through analytical theory [2], [3], particle-in-cell (PIC) simulations [4], [5], [6], [7], [8] and laboratory experiments [9], [10]. HPM Vacuum Electronic Devices (HPMVEDs) driven by intense electron beams produce the highest achievable levels of controlled output electromagnetic power in the very broad frequency range spanning from hundreds of MHz in ultra-high-frequency band, to hundreds of GHz in millimeter-wavelength and terahertz-frequency bands.

HPMVEDs of different kinds and flavors are used nowadays almost everywhere, from nuclear fusion research experiments to heat plasmas at electron cyclotron resonance [11] to directed energy military applications to disrupt and destroy electronic circuits with high oscillating electric fields [12]. Electromagnetic power is generated inside HPMVEDs in a high vacuum as a result of energy exchange between moving electrons, whose movement is usually confined by external and internal electric and magnetic as well electromagnetic fields, and a "seed" electromagnetic field, which is either externally injected into a HPMVEDs or just grows from the electromagnetic noise always existing inside a HPMVED as a result of electron movement. Correct understanding of the entire mechanism of electromagnetic energy exchange between (i) electrons moving inside a HPMVED, and (ii) infinitely large number of electromagnetic modes possible to exist inside a HPMVED is necessary. This understanding brings unprecedented scientific advances and produces great impact on the design and development of novel, more powerful and better controlled sources of output electromagnetic power.

UNM operates two very different pulsed-power sources (Fig. 1), a PULSERAD PI-110A built around a "Marx" generator [13]; and a SINUS-6 built around a "Tesla" transformer [14], [15], [16], each of which is capable of producing up to 10-30-ns duration electron beams in different HPMVEDs driven by accelerating voltages up to ~700 kV and electron-beam currents up to ~4 kA, depending on the configuration of the HPMVED. This paper describes the current status of UNM research activity on one HPMVED – six-cavity "classical 1.58/2.11/4.11 relativistic or high-voltage magnetron, where 1.58, 2,11, and 4.11 indicate, respectively, radii of cathode, anode, and cavity in cm – driven by the PULSERAD PI-110A pulsed-power source.

The UNM A6 magnetron is designed and built in two basic configurations of output electromagnetic/microwave power extraction from its resonant cavities (Fig. 2). One "classical" configuration of the magnetron provides radial output of microwave power extraction from one of six resonant cavities into a rectangular horn antenna. Another configuration provides diffraction output of microwave power extraction from all six resonant cavities in the axial direction, either immediately onto a smooth-walled cylindrical waveguide gradually transformed into a conical horn antenna, or smoothly through a tapered, in the axial direction, slow-wave structure (SWS) of the magnetron also gradually transformed then onto a smooth-walled cylindrical waveguide terminated in a conical horn antenna. In both configurations, while driven by the kV/kA PULSERAD PI-110A, the A6 magnetron is able to provide hundreds of MW of output microwave power, either in the 2π-mode or in the π-mode. The "cold" operational frequency of the 2π-mode is ~4.6 GHz and the "cold" operational frequency of the π-mode is ~2.3 GHz with a standard solid cylindrical "cold" explosive-emission cathode. The cathode is a source of an electron flow produced by an accelerating high-voltage pulse supplied by the PULSERAD PI-110A.

The results of the latest experimental measurements of the main operational parameters of the PULSERAD-110A / A6 magnetron HPM system, where the output microwave power is extracted from radial output of the magnetron through ATM WR-229/284 waveguide transition into WR-229 horn antenna and allows us to conclude that:

1. Experimentally measured frequency of A6 magnetron operation is 4.68-4.69 GHz (Fig. 3) which means that it works in the 2π-mode, with the microwave pulse duration ~25 ns. The operating frequency of the magnetron is determined by FFT/STFT analyses using OriginPro Data Analysis and Graphing Software from electric field pulses measured by a PRODYN Technologies MODEL BIB-100G electric field probe located at distance ~3 m from the output microwave window of the WR-229 horn antenna (Fig. 4), and connected through ~50

ft long Pasternack RG-214/U coaxial cable into a KEENE Corporation RF Shielded Room to a 50 Ω Tektronix MSO-71604C oscilloscope where the signal is acquired and digitized.

Fig. 1. UNM Pulsed Power, Beams and Microwaves Laboratory with PULSERAD PI-110A (left) and SINUS-6 (right) pulsed power sources.

a)

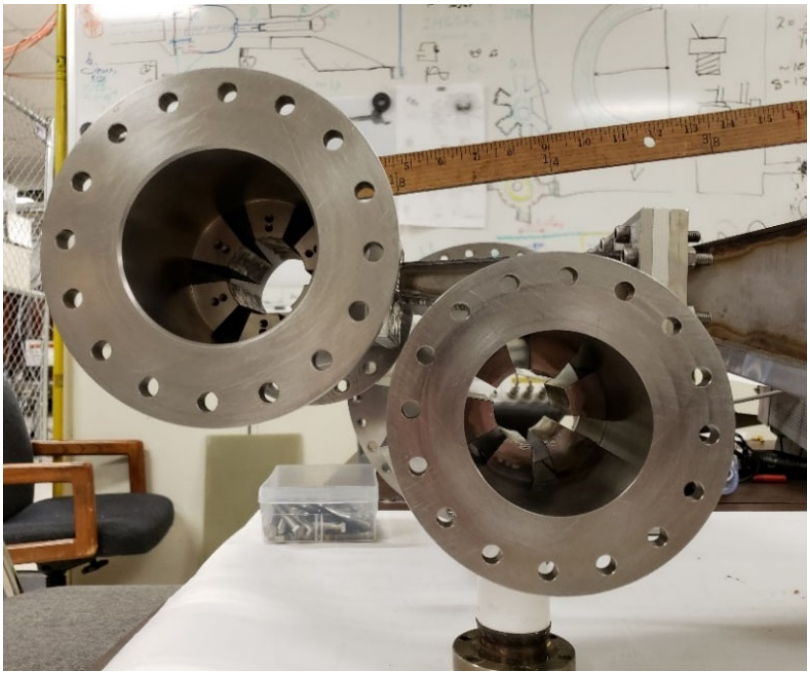

b)

Fig. 2. UNM A6 magnetrons: (a) side view of both magnetrons with axial output (left)) and radial output (right) of microwave power, (b) axial view of both SWS with radial (left) and axial (right) outputs of microwave power.

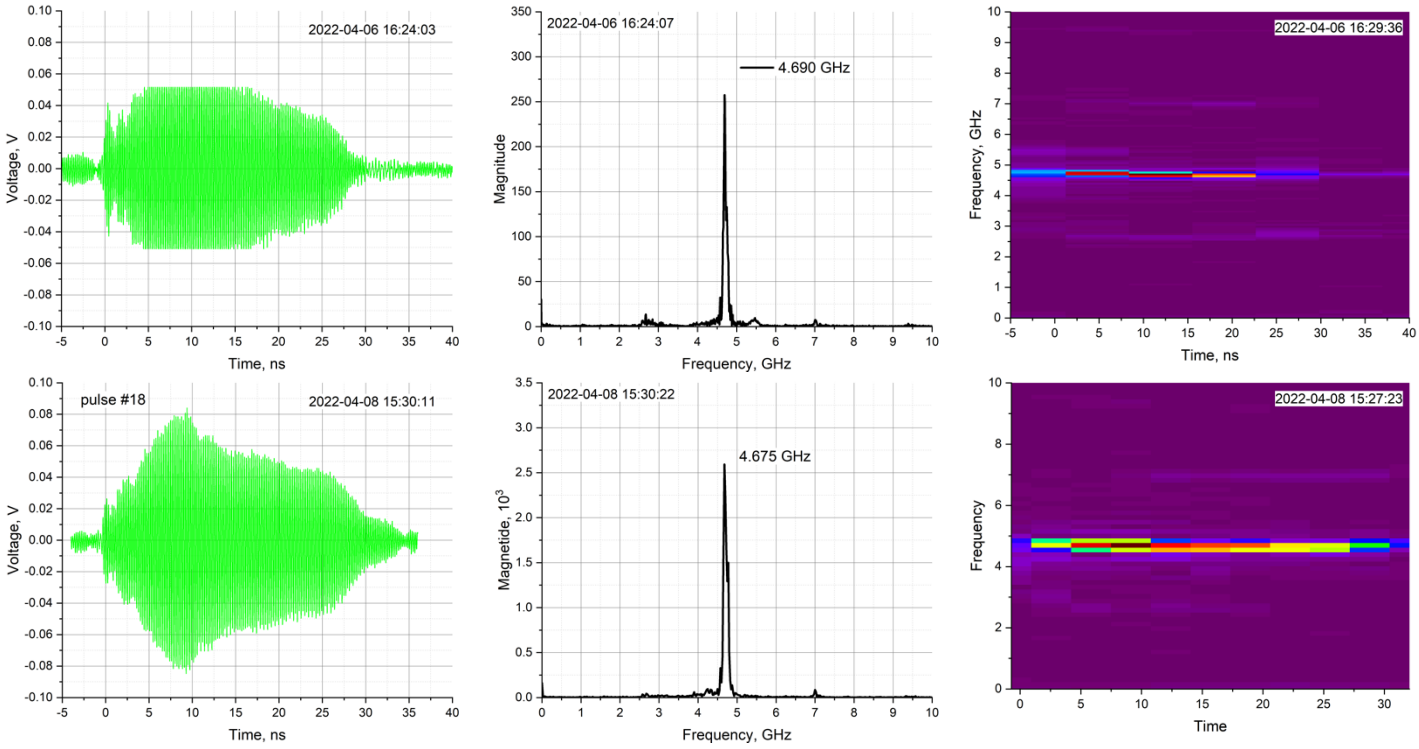

Fig. 3. Measured electric field pulses: (left) oscillograms, (central) FFT, and (right) STFT of oscillograms.

Fig. 4. Experimental measurements of operating frequency of UNM A6 magnetron: a) general view, b) radial output of microwave power through WR-229 waveguide rectangular horn antenna, c) and d) electric field probe used for measurements of operating frequency.

2. Experimentally measured output microwave power of the magnetron is ~350 MW, which is a moderate value for the 2π-mode operation of a standard A6 magnetron at accelerating voltages ≤250 kV. The output microwave power is sampled by a MEGA/RF WR-229 Reflectometer, with -70 dB @ 4.675 GHz of "forward power flow (Fig. 5)," inserted between the radial output of the magnetron with in-series ATM WR229/WR284 waveguide-to-waveguide transition adapter, and a WR-229 horn antenna (Fig. 6). The sampled output microwave power is provided through a ~50 ft long Coleman RG-214/U coaxial cable, -21 dB @ 4.675 GHz, and an additional in-series set of Pasternack coaxial attenuators, -17 dB @ 4.675 GHz, is connected to an input port of a NARDA 501B crystal detector (Fig. 7(a)) This output signal is acquired by a 1 MΩ Tektronix TDS 350 oscilloscope in the Shielded Room. Measurements of the Input Power (dBm) / Output Voltage (mV) "response curve" of the NARDA 501B crystal detector (Fig. 7(b)) is done with an HP 83752B synthesized sweeper and a 1 MΩ TDS 350 oscilloscope (Fig. 8). Calibration of the WR-229 Reflectometer, RG-214/U cable, and Pasternack attenuators at the operating frequency 4.675 GHz is done with a Keysight PNA-L N5235A Network Analyzer (Fig. 9).
3. Experimentally measured oscillograms of Output Voltage (mV) from the NARDA 501B crystal detector (Fig. 7(a)) and oscillograms of accelerating voltage pulse (V) supplied by the PULSERAD- PI-110A are shown in Fig. 10. Oscillograms of accelerating voltage, Ch#1 in Fig. 10, are obtained by integrating the signal monitored by the *V-dot* probe located on the cathode holder of the A6 magnetron (Fig. 11). Instrumental integration of the *V-dot* probe signals into real oscillograms of accelerating voltage (Fig. 12) is performed using in-series integrators (Fig. 13) borrowed from Dr. M. Collins Clark, Collins Clark Technologies (CCT) Inc., Albuquerque, NM.

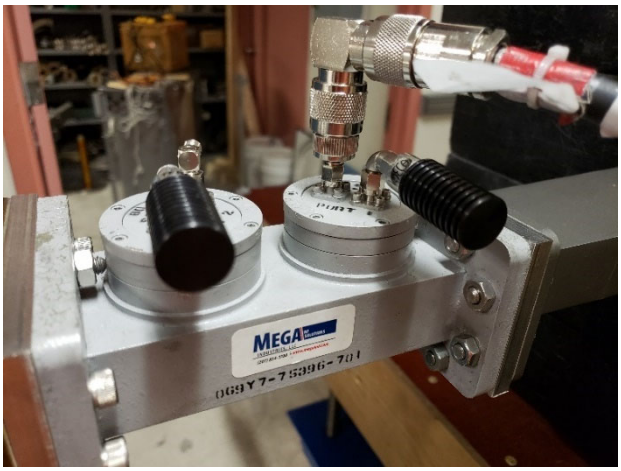

Fig. 5. MEGA/RF WR229 Waveguide Directional Coupler/Reflectometer.

Fig. 6. ATM WR229/WR284 waveguide-to-waveguide transition adapter.

a)

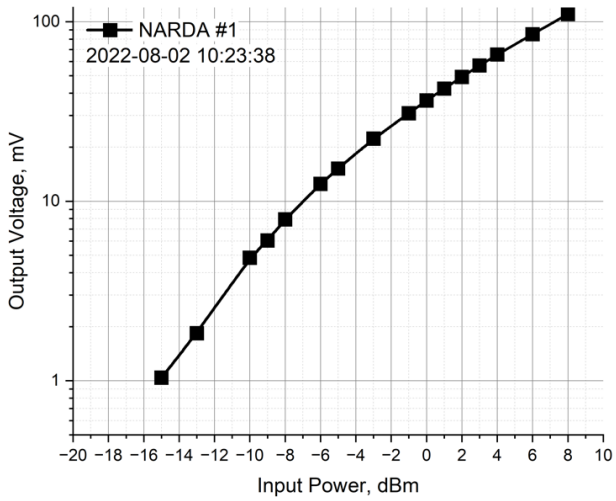

b)

Fig. 7. a) two crystal detectors NARDA 501B, and b) measured "square-low" response of crystal detector #1.

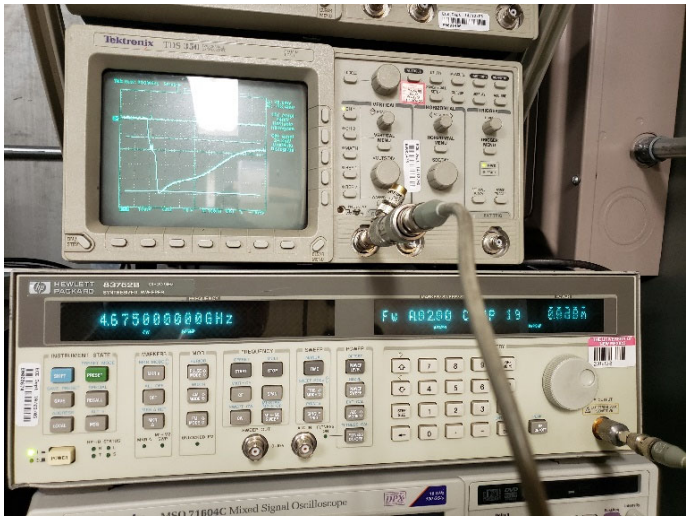

a)

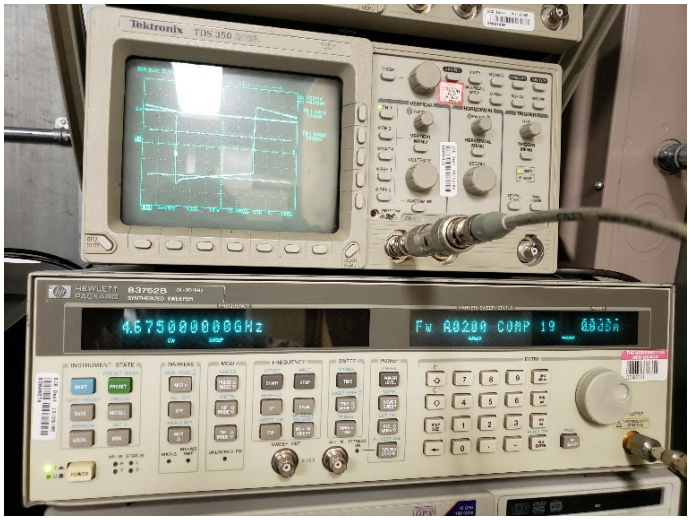

b)

Fig. 8. Calibration of NARDA 501B crystal detectors
with HP 83752B synthesized sweeper (RF generator) and TDS 350 oscilloscope:
a) 50 Ω in parallel to 1 MΩ oscilloscope input, and 2) 1 MΩ oscilloscope input.

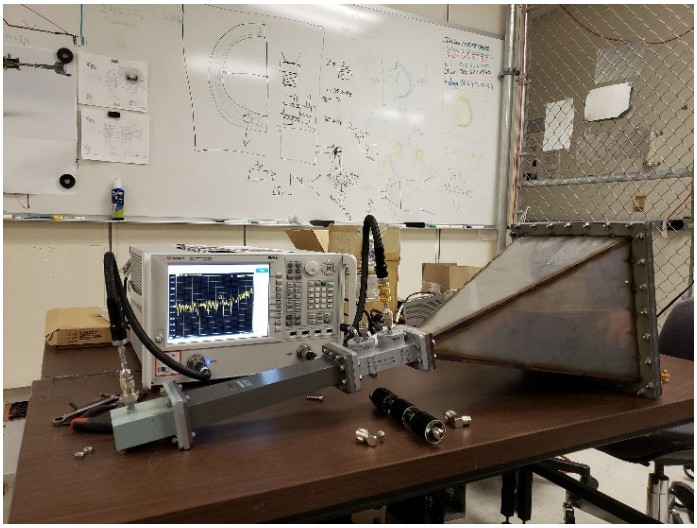

c)

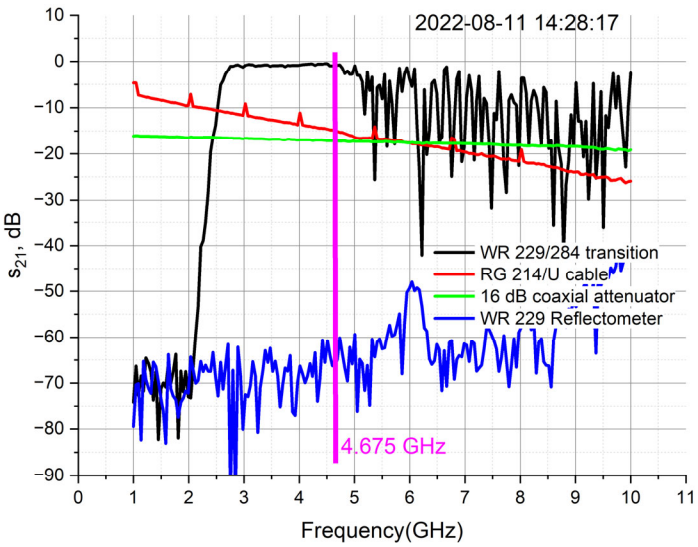

d)

Fig. 9. Measurements of s_{21} parameters. of WR 229/284 waveguide transition and WR 229 Reflectometer.

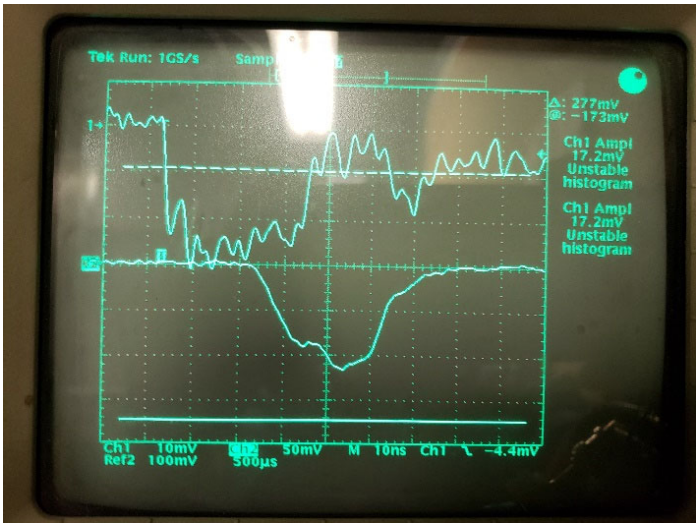

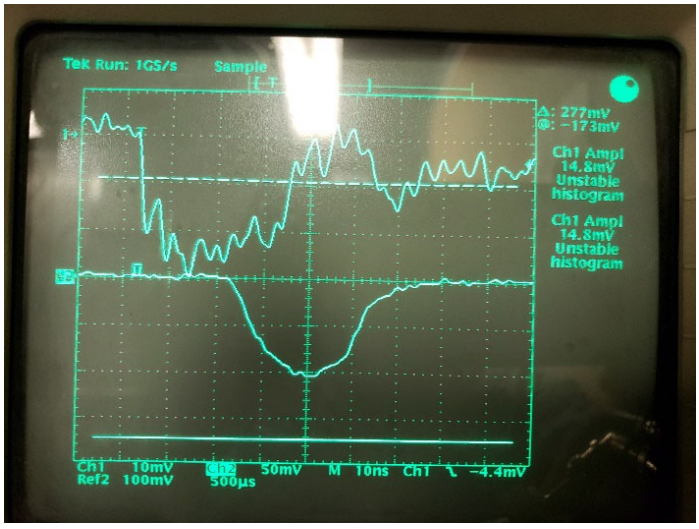

Fig. 10. Measured oscillograms of output voltage from voltage integrator, Ch#1, and output voltage from NARDA 501B crystal detector, Ch#2.

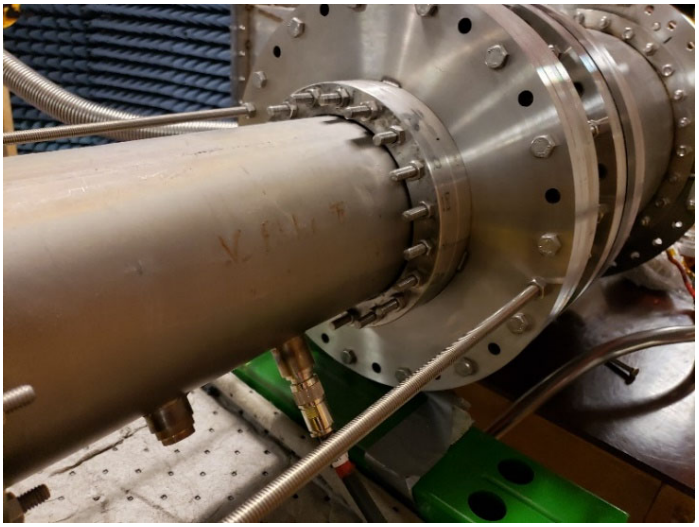

Fig. 11. D-dot probe near cathode shank of A6 magnetron.

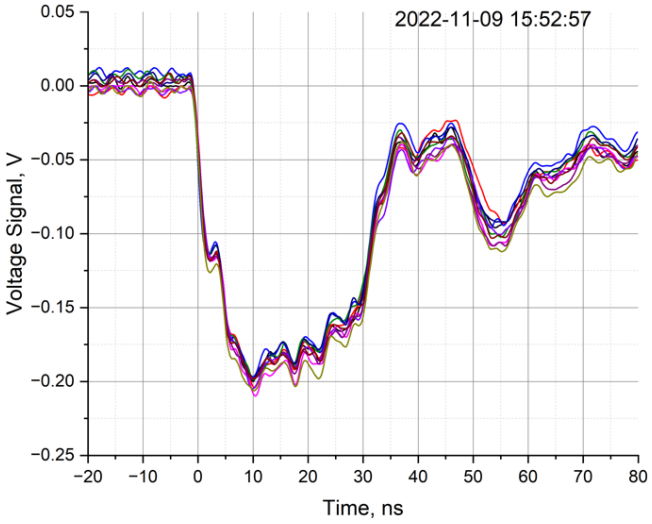

Fig. 12. Ten sequential pulses of voltage measured near cathode shank of A6 magnetron (Fig. 11) and integrated by Collin's integrator.

a)

b)

Fig. 13. Collins' integrators used to integrate *V-dot* probe signals measured on cathode holder of A6 magnetron: a) just a two of them, and b) oscilloscope input.

Assuming that the measured signal from the NARDA 501B crystal detector (Fig. 7(a)) is ~100 mV (Fig. 10), which corresponds to ~7.5 dBm of input power to the crystal detector (Fig. 7(b)), and that the measuring circuit from radial output of A6 magnetron (Fig. 5) to the NARDA 501B crystal detector (Fig. 11(b)) includes (Fig. 9(d)): (i) ~70 dB directional coupler, (ii) ~17 dB coaxial attenuator, and (ii) ~21 dB "RF" Cable#1, the total measured microwave power of A6 relativistic magnetron at operating frequency 4.675 GHz is recalculated into ~350 MW, as it follows from (1). Output microwave power of ~350 MW from the radial output of the A6 relativistic magnetron is a quite reasonable value, assuming that both magnetic field strength and accelerating voltage amplitude are to be calibrated yet.

$$10^{-3}\cdot 10^{\frac{7.5}{10}} = 5.623\times 10^{-3}\ ;\ 5.623\times 10^{-3}\cdot 10^{\frac{17+21+70}{10}} = 3.548\times 10^{8} \qquad (1)$$

UNM continues its analytical theory development [2], [3], particle-in-cell (PIC) simulations [4], [5], [6], [7], [8] and laboratory experiments [9], [10] aiming further study of the A6 relativistic magnetron operation with both radial and axial outputs of microwave power (Fig. 2) by performing the following activities:

- experimental measurements of operating frequency and output power of the A6 relativistic magnetron with radial output of microwave power using a WRF-284 directional coupler, a WR-284 rectangular horn antenna, and a crystal detector with a 1 MΩ Tektronix TDS 350 oscilloscope input;
- calibration of all the measuring circuits and instruments to provide an accurate monitor of both the magnetic field strength and the accelerating voltage applied to the A6 relativistic magnetron in real-time experimental measurements of output operational parameters of the magnetron. There will be no substantial efforts implemented to measure the total discharge current of the magnetron. This is because the anode current of a magnetron is not a space-charge limited current of electrons in a coaxial diode, but a voltage-controlled electron-drift current in crossed quasi-state axial magnetic field and oscillating azimuthal electric field of magnetron oscillations. The electron drift current inside a slow-wave structure of a magnetron is technically impossible to measure experimentally;
- ICEPIC simulations of operational parameters of the A6 relativistic magnetron with radial output of microwave power within experimentally achievable by the PULSERAD-110A and technically reasonable ranges of magnetic fields and accelerating voltages and correlation of computational results with results of experimental measurements. The Improved Concurrent Electromagnetic Particle-in-Cell (ICEPIC) code may be run either in-house on powerful desktop Linux boxes or using remote DoD Supercomputing Resource Centers (DSRC) through the DoD High Performance Computing Modernization Program (HPCMP);
- experimental measurements of the operating frequency the A6 relativistic magnetron with axial or diffraction output of microwave power and ICEPIC simulations of all main operational parameters of the A6 relativistic magnetron.

The concept of the Magnetron with axial output of microwave power, which is also known as the Magnetron with Diffraction Output (MDO), is based on an inner architecture of a conventional magnetron SWS with radial output power (Fig. 14(a)). The MDO is re-designed in such a way that the radial output of microwave power is eliminated and either all cavities and vanes of the SWS or just some of them are smoothly tapered in the axial direction onto a conical horn antenna that is designed for the axial output of the microwave power (Fig. 14(b,c)) [6], [7], [8]. The tapered (in the axial direction) cavities and vanes of the SWS define the topology of an electromagnetic mode transformer build into the conical horn antenna.

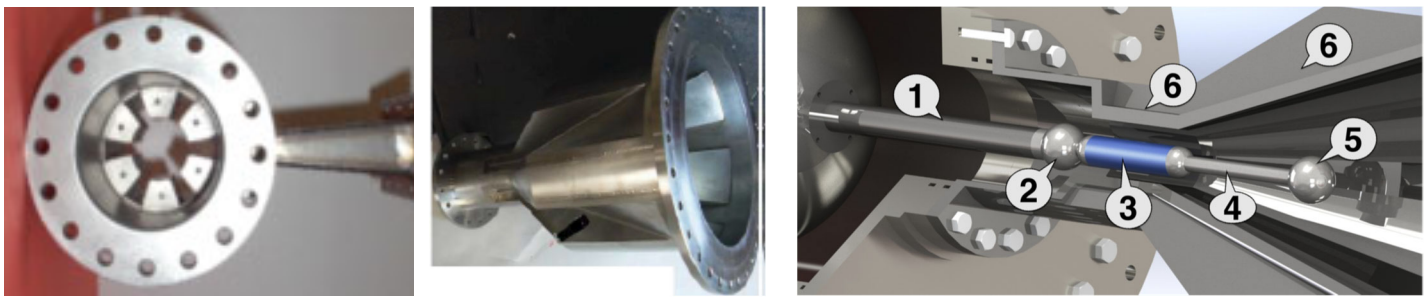

a) b) c)

Fig. 14. Magnetron with diffraction output of microwave power: a) A6 relativistic magnetron with radial output designed and built at UNM, b) A6 MDO designed and built at UNM, c) schematic of A6 MDO designed and built at UNM, where (1) cathode holder, (2) upstream endcap, (3) solid cylindrical cathode with emission area in blue, inside the magnetron interaction region or SWS, (4) connecting rod, (5) downstream endcap, and (6) anode or SWS of the magnetron.

UNM is working now on studying the operation of the A6 MDO (Fig. 2, (Fig. 14). The optimized design of the diffraction microwave power output (Fig. 14(b,c)) with appropriate built-in electromagnetic mode transformer transforms the "*donut-like*" radiation pattern of the MDO operating in a TE_{n1} mode (Fig. 15(a)), where n=3 is half of a number of the A6 magnetron resonators, into the Gaussian-like TE_{11} mode with n=1 (Fig. 15(b)). This radiation pattern (Fig. 15(b)) is more effective for both DE and non-DE HPM/HPEM applications.

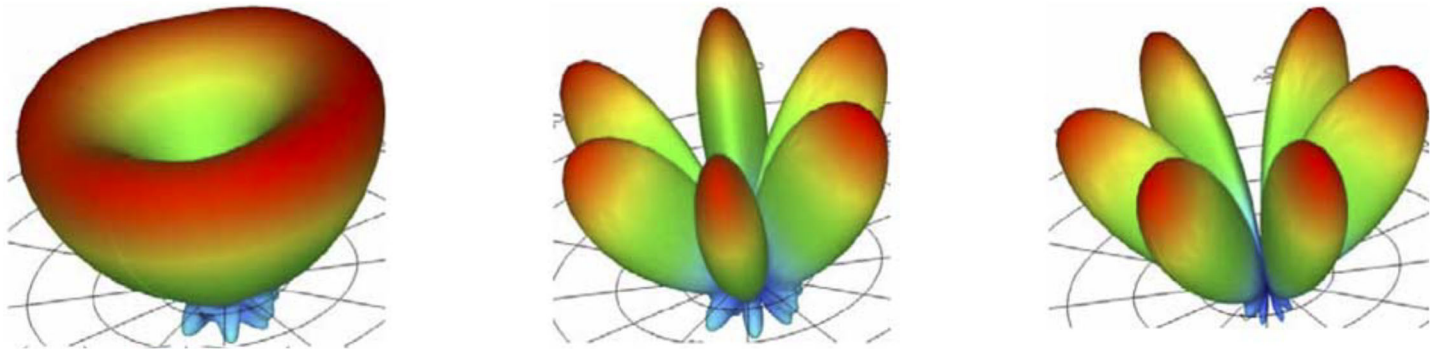

a)

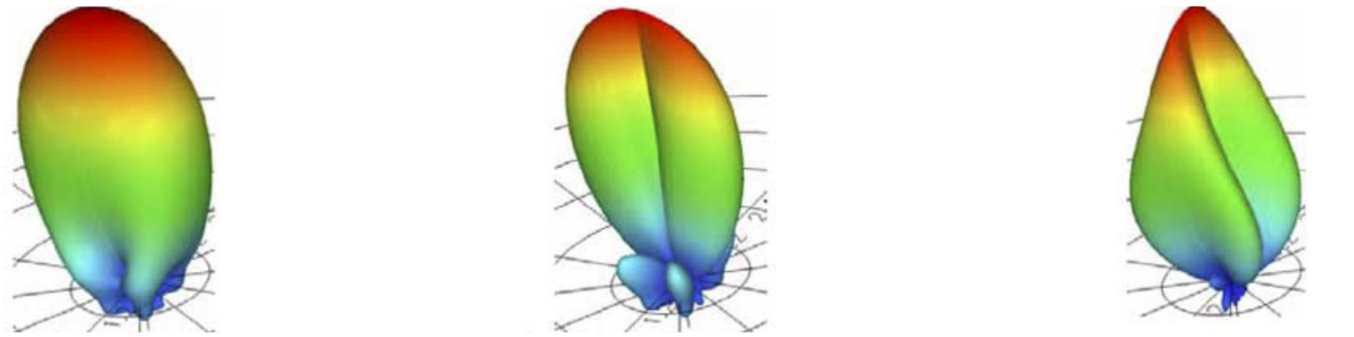

b)

Fig. 15. Calculated far-field distributions of output microwave power produced by a 6-resonator MDO, when: a) all six resonators are tapered in axial direction onto a conical horn antenna radiating TE_{31} mode, and b) only three alternating resonators are tapered in axial direction onto a conical horn antenna radiating TE_{11} Gaussian-like mode. From left to right are the following components of the far-field distribution: left - $|E|$, center - $|E_\theta|$, and right - $|E_\varphi|$.

Conclusion:

The above-described UNM laboratory experiments on advancing intense electron-beam-driven HPM sources, of which a relativistic magnetron is the most compact and effective HPMVED, are accompanied by virtual prototyping and numerical simulation of such HPMVEDs with modern computer codes of different purposes. Computer simulations of HPMVEDs with Particle-in-cell (PIC) are performed to design, research and develop novel, more efficient and agile, higher power / longer pulse duration / higher repetition rate HPM sources. The PIC simulations of HPMVEDs require enormous computational resources in terms of node-hours. This is why all modern PIC codes are designed to operate on high-performance computers (HPC) clusters using parallel computing architectures.

UNM employs the Improved Concurrent Electromagnetic Particle-In-Cell (ICEPIC) code for virtual prototyping, numerical modeling and simulations of modern and prospective HPMVEDs, including relativistic magnetrons. The ICEPIC code, developed at the Air Force Research Laboratory, Directed Energy Directorate, High-Power Electro-magnetic Division, is a PIC code specifically designed for parallel high-performance computing resources. The ICEPIC code is the right tool to solve all possible technical challenges UNM expects to face. It provides the self-consisted electromagnetic and PIC simulations arising due to the non-linear nature of HPMVEDs operating in extreme electromagnetic field environments.

The ICEPIC code is a relativistic, 3-D Cartesian/Cylindrical, variable mesh, electromagnetic, parallel PIC code capable of simulating collisionless plasma physics phenomena governing a wide variety of electromagnetic problems, including high-power microwave/millimeter-wavelength VEDs operation. It was specifically designed to take advantage of the latest parallel high-performance computing (HPC) resources. ICEPIC is written in ANSI-C and uses the industry standard message passing interface (MPI). The ICEPIC's parallel design and portability ensure that it is scalable and capable of efficiently executing on a variety of HPC architectures.

References:

[1] S. D. Korovin et al., "Pulsed power-driven high-power microwave sources," in *Proceedings of the IEEE*, vol. 92, no. 7, pp. 1082-1095, July 2004, doi: 10.1109/JPROC.2004.829020.

[2] A.D. Andreev, K.J. Hendricks, M.I. Fuks, and E. Schamiloglu, "Elemental theory of a relativistic magnetron operation: Anode current," in *Journal of Directed Energy*, Vol. 3, No. 4, Summer of 2010, pp. 349-383.

[3] A.D. Andreev, K.J. Hendricks, S. Soh, M. Fuks, and E. Schamiloglu, "Elemental theory of a relativistic magnetron operation: Dispersion diagram," in *Journal of Directed Energy*, Vol. 5, No. 1, Spring of 2013, pp. 1-41.

[4] Mikhail Fuks and Edl Schamiloglu, "Rapid Start of Oscillations in a Magnetron with a "Transparent" Cathode," *Physical Review Letters*, Volume 95, Number 20, 11 November 2005, pp. 205101(4).

[5] Herman L. Bosman, Mikhail Fuks, Sarita Prasad and Edl Schamiloglu, "Improvement of the Output Characteristics of Magnetrons Using the Transparent Cathode," *IEEE Transactions on Plasma Science*, Volume 34, Number 3, June 2006, pp. 606-619.

[6] M. I. Fuks, N. F. Kovalev, A. D. Andreev and E. Schamiloglu, "Mode conversion in a magnetron with axial extraction of radiation," in *IEEE Transactions on Plasma Science*, vol. 34, no. 3, pp. 620-626, June 2006, doi: 10.1109/TPS.2006.875770.

[7] M. I. Fuks and E. Schamiloglu, "70% Efficient Relativistic Magnetron with Axial Extraction of Radiation Through a Horn Antenna," in *IEEE Transactions on Plasma Science*, vol. 38, no. 6, pp. 1302-1312, June 2010, doi: 10.1109/TPS.2010.2042823.

[8] C. Leach, S. Prasad, M. I. Fuks and E. Schamiloglu, "Compact Relativistic Magnetron with Gaussian Radiation Pattern," in *IEEE Transactions on Plasma Science*, vol. 40, no. 11, pp. 3116-3120, Nov. 2012, doi: 10.1109/TPS.2012.2212910.

[9] C. Leach, S. Prasad, M. I. Fuks and E. Schamiloglu, "Suppression of Leakage Current in a Relativistic Magnetron Using a Novel Design Cathode Endcap," in *IEEE Transactions on Plasma Science*, vol. 40, no. 8, pp. 2089-2093, Aug. 2012, doi: 10.1109/TPS.2012.2199136.

[10] C. Leach, S. Prasad, M. I. Fuks, J. Buchenauer, J. W. McConaha and E. Schamiloglu, "Experimental Demonstration of a High-Efficiency Relativistic Magnetron with Diffraction Output with Spherical Cathode Endcap," in *IEEE Transactions on Plasma Science*, vol. 45, no. 2, pp. 282-288, Feb. 2017, doi: 10.1109/TPS.2016.2644625.

[11] Hyeon K. Park, "Role of Radio Frequency and Microwaves in Magnetic Fusion Plasma Research," in *J. Electromagn. Eng. Sci*., 2017, Vol. 17, No. 4, pp. 169-177. Published online October 31, 2017, DOI: https://doi.org/10.26866/jees.2017.17.4.169.

[12] "High-Power Microwave Systems – Getting (Much, Much) Closer to Operational Status" by Barry Manz, in *Journal of Electromagnetic Dominance*, January 2023, Vol. 46, No. 1, pp. 16-20.

[13] K. Hahn, M. I. Fuks and E. Schamiloglu, "Initial studies of a long-pulse relativistic backward-wave oscillator utilizing a disk cathode," in *IEEE Transactions on Plasma Science*, vol. 30, no. 3, pp. 1112-1119, June 2002, doi: 10.1109/TPS.2002.801628.

[14] L. D. Moreland, E. Schamiloglu, R. W. Lemke, S. D. Korovin, V. V. Rostov, A. M. Roitman, K.J. Hendricks and T.A. Spencer, "Efficiency enhancement of high-power vacuum BWO's using nonuniform slow wave structures," in *IEEE Transactions on Plasma Science*, vol. 22, no. 5, pp. 554-565, Oct. 1994, doi: 10.1109/27.338268.

[15] E. Schamiloglu, R. Jordan, M. D. Haworth, L. D. Moreland, I. V. Pegel and A. M. Roitman, "High-power microwave-induced TM_{01} plasma ring," in *IEEE Transactions on Plasma Science*, vol. 24, no. 1, pp. 6-7, Feb. 1996, doi: 10.1109/27.491664.

[16] L. D. Moreland, E. Schamiloglu, R. W. Lemke, A. M. Roitman, S. D. Korovin and V. V. Rostov, "Enhanced frequency agility of high-power relativistic backward wave oscillators," in *IEEE Transactions on Plasma Science*, vol. 24, no. 3, pp. 852-858, June 1996, doi: 10.1109/27.533088.